

Fabrication and Research of Superhard (Zr–Ti–Cr–Nb)N Coatings

O.V. BONDAR^a, B.O. POSTOLNYI^{a,*}, YU.A. KRAVCHENKO^a, A.P. SHYPYLENKO^a,
O.V. SOBOL^b, V.M. BERESNEV^c, A.P. KUZMENKO^d AND P. ZUKOWSKI^e

^aSumy State University, R. Korsakova 2, 40007 Sumy, Ukraine

^bNational Technical University “Kharkiv Polytechnic Institute”, Kharkiv, Ukraine

^cKharkiv National University, Kharkiv, Ukraine

^dSouth-West State University, Kursk, Russian Federation

^eDepartment of Electrical Devices and High Voltage Technology, Lublin University of Technology, Lublin, Poland

This work presents the results of (Zr–Ti–Cr–Nb)N superhard coatings research. The samples were fabricated by the vacuum-arc deposition method (Arc-PVD). Structure, composition and properties of these coatings were studied. The study of coatings was carried out using scanning electron microscopy, energy dispersive spectroscopy, and X-ray diffraction. Hardness measurements and adhesion tests were performed. The coatings thickness was up to 6.2 μm , nanocrystallites sizes ranged from 4 to 7.3 nm. Values of hardness and cohesive strength were $H = 43.7$ GPa and $L_C = 62.06$ N, respectively. The optimal conditions for coating deposition were found.

DOI: [10.12693/APhysPolA.128.867](https://doi.org/10.12693/APhysPolA.128.867)

PACS: 61.46.–w, 62.20.Qp

1. Introduction

The nitride coatings based on the transition metals such as TiN, ZrN, CrN, NbN and others are intensively used in various branches of industry nowadays (aerospace machines, different biomedical applications, treatment of cutting tools, diffusion barriers in modern electronics, etc.) [1–6]. Ternary and quaternary nitride systems are under great interest because of their unique combination of structural characteristics and exceptional mechanical properties, wear-corrosion-oxidation resistance. For example, ternary nitride coatings are produced by addition of a third element such as V, Al, Nb, Zr etc. to a binary nitride compounds (e.g. TiN, MoN, VN, ZrN, CrN, AlN, NbN). A small quantity of the third element significantly changes the morphology, structure, physical and mechanical properties of the coatings [7–10]. Quaternary coatings of the above systems, such as Ti–Al–Si–N, Zr–Nb–Ti–Cr–N, Zr–Ti–Cr–N and others are also of great interests [11]. Minor addition of alloying elements into binary and ternary nitride system provide a further improvement of coatings properties and structure. For example, if the constituent elements have significant differences in atomic radii, we can expect the formation of nanocrystalline structures. The presence of alloying elements such as Cr improves the oxidation resistance, Zr and V contribute to a better wear resistance, whereas Nb increase the hardness and thermal stability [12–14].

It should be noted that the magnetron sputtering is one of the most widely used techniques for

the multicomponent nitride coatings deposition. In this paper, the vacuum arc deposition was used for the preparation of nitride coatings. Good advantage of this method is its ability to generate a much higher degree of ionization than other ion-plating processes, providing a better film adhesion and higher densities.

The goal of this paper is to study the structure and properties of (Zr–Ti–Cr–Nb)N coatings, fabricated by vacuum arc deposition. The influence of deposition parameters on the microstructure and properties of the films are investigated and discussed.

2. Experimental details

Coatings of (Zr–Ti–Cr–Nb)N system were fabricated using the vacuum-arc deposition method (Arc-PVD). The samples were deposited in nitrogen atmosphere using the vacuum-arc device “Bulat-6” [13]. The evaporated material was a cast in block Zr+Ti+Cr+Nb cathode (composition: Cr — 37.39 at.%, Zr — 27.99 at.%, Nb — 22.30 at.%, Ti — 12.32 at.%) fabricated by electron-beam melting. Table I shows physical and technological parameters of coatings fabrication based on the (Zr–Ti–Cr–Nb)N system.

Surface morphology of coatings and their elemental composition were studied using the scanning electron microscope JEOL-6610 LV equipped with a built-in energy dispersive analyzer (X-Max Silicon Drift Detector). The crystal structure and phase composition were analyzed by the X-ray diffraction (XRD) with D8 ADVANCE and DRON-4 diffractometers using Cu K_α irradiation. The XRD patterns were taken in the point-by-point scanning mode with the scanning step $2\theta = 0.02$ – 0.2° in the range of angles 25 – 90° .

*corresponding author; e-mail: alexp@i.ua

TABLE I

Deposition parameters and elemental composition of coatings.

Sample No	I_a [A]	p_N [Pa]	U_b [V]	Concentration [at. %]							
				Ti	Zr	Cr	Nb	N	C	O	Impurities
1	110	0.3	-100	10.21	6.63	15.22	4.96	18.70	38.29	5.42	0.57
2		0.7	-100	12.30	8.48	16.92	6.17	22.32	27.35	6.46	–
3		0.3	-200	11.27	8.03	18.23	7.48	23.20	31.79	–	–
4		0.7	-200	10.40	7.81	11.00	6.73	22.66	35.63	5.37	0.39

Microhardness of coatings was measured by automated Vickers hardness tester AFFRI DM-8. The imprints were made at the distance of 1.0 mm between each other, 10 measurements were held for each sample. In order to reduce the impact of droplet component and in order to measure the hardness of the coatings more accurately, some coatings had been polished after deposition.

Studying of mechanical characteristics (hardness) of the (Zr–Ti–Cr–Nb)N coatings was carried out by a DM-8 hardness tester. The imprints were made at the distance of 1.0 mm between each other, ten measurements were held for each sample. In order to reduce the impact of droplet component, part of the coatings were polished after deposition. Scratch-tester Revetest (CSM Instruments) was used for adhesion strength study. The scratches were made on the surface of the coated samples at continuously increasing load by means of the diamond spherical indenter “Rockwell C” type with a radius of curvature of 200 μm and there were registered the following physical parameters: acoustic emission, coefficient of friction and depth of penetration of the indenter. To obtain the reliable results, two scratches on the surface of the coating were made.

The following critical loads changing the coefficient of friction and acoustic emission curves from the scribing load are: L_{C1} — characterizes the time of occurrence of the first chevron crack; L_{C2} — the moment of the appearance of chevron cracks; L_{C3} — the destruction of cohesive and adhesive nature; L_{C4} — the local flaking of the areas of the coating; L_{C5} — the plastic abrasion of the coating to the substrate.

3. Results and discussion

Figure 1 present the SEM images of the (Zr–Ti–Cr–Nb)N coatings. One can see molten droplets there, which may be incorporated into the coating as macroparticles; it is typical during vacuum arc deposition [15–18]. As we can see from Fig. 1, the (Zr–Ti–Cr–Nb)N coating contains inclusions of a droplet fraction up to 6 μm in diameter. Such microdroplets have ellipsoidal shape, which indicates that they moved almost parallel to the substrate plane. An increase of the deposition flow temperature using high bias voltage ($U = -200$ V) considerably decreased a droplet concentration on the surface (see Fig. 1b). The reduced content of droplets can be explained by melting processes on the coating’s surface.

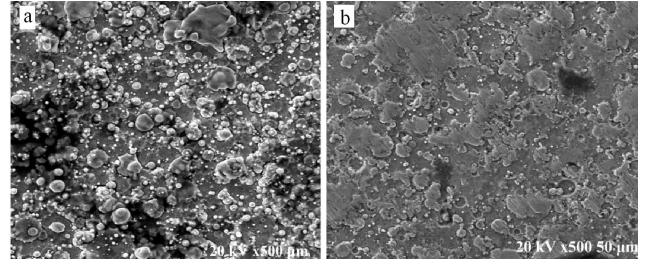


Fig. 1. SEM-images of the (Zr–Ti–Cr–Nb)N coatings: (a) $P_N = 0.3$ Pa, $U = -100$ V; (b) $P_N = 0.7$ Pa, $U = -200$ V.

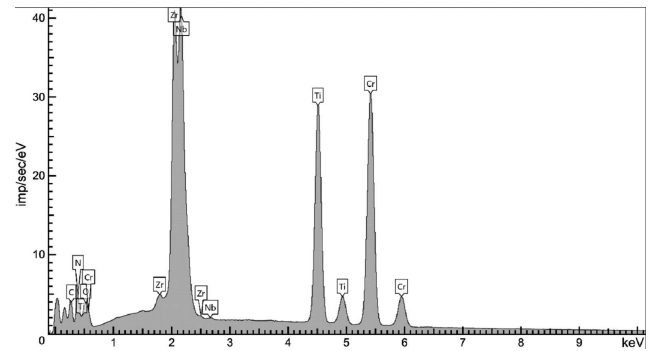


Fig. 2. Energy-dispersive X-ray spectrum (sample #2).

The elemental analysis shows that the ratio of elements in the composition of material has the same tendency in all obtained coatings: $C_C > C_N > C_{Cr} > C_{Ti} > C_{Zr} > C_{Nb} > C_{\text{impurities}}$. Detailed elemental compositions of samples #1–4 are listed in Table I. The energy-dispersive X-ray spectrum obtained from the sample #2 (see Fig. 2) confirms the existence of elements presented in Table I.

TABLE II

Size (L) and lattice constants of crystallites (for fcc lattice).

Sample	1	2	3	4
grain size, L [nm]	5.2	4.5	5.1	6.9
lattice constant [nm]	0.4365	0.4359	0.4410	0.4381

The phase analysis of (Zr–Ti–Cr–Nb)N nitride coatings using XRD is presented in Fig. 3. It indicates the presence of the TiN fcc phase ($a = 0.243$ nm,

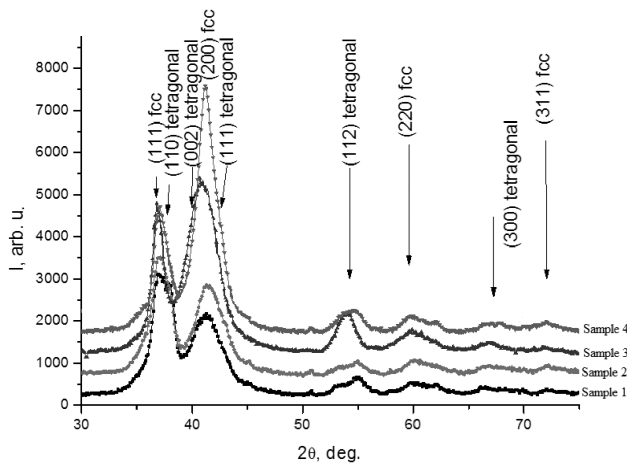


Fig. 3. X-ray diffraction patterns obtained for samples #1–4.

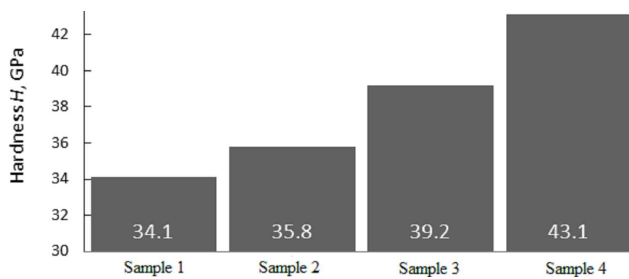


Fig. 4. Results of microhardness measurements of the coatings.

$a_{\text{tab}} = 0.244$ nm) and Cr_2N tetragonal modification (space group $P31m$, $a = 0.4800$ nm, $c = 0.4472$ nm). The formation of a two-phase structure is obviously related to the presence of high concentrations of Cr and Nb elements, which have a low enthalpy of formation of nitrides [19]. The substrate *bias* strongly influences the orientation changing from preferred (111) to mixed (111) and (200) ones, and the appearance of the (112) and (300) reflections at high angles (Cr_2N tetragonal phase). It is worth saying that the maximum intensity of the (112) and (300) reflections corresponds to the highest concentration of Cr in the coating [13, 17]. Table II lists the grain size and lattice parameters of the (Zr–Ti–Cr–Nb)N coatings, which were further evaluated from the XRD patterns. This table reveals that the lattice constant increases with bias increasing. This is reasonable because the energetic bombardment causes incorporation of nitrogen atoms into the spaces in the growing coating that are smaller than the usual atomic volume (so called “atomic peening effect”) [20–22]. Additionally, the grain size of the (Zr–Ti–Cr–Nb)N nitride coatings is around 5.5 nm under all of various biases, which means that deposited coatings have fine nanocrystalline structures.

Microhardness measurements of the investigated samples are presented in Fig. 4. Growth of microhardness

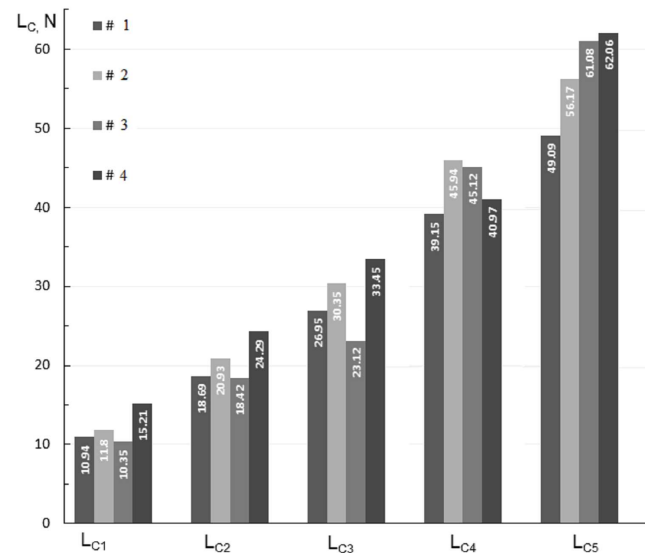


Fig. 5. Results of adhesion tests of the investigated coatings.

observed in the coatings with a larger crystallite size which were fabricated at higher nitrogen pressure and bias potential. In addition, sample #4 became a leader in the adhesive tests (see Fig. 5). Comparative analysis shows that the coatings are erased, but not peeled during scratching. That is cohesive failure associated with plastic deformation [23–25], and formation of fatigue cracks in the coating’s material takes place. The cohesive strength of multi-component coating (Zr–Ti–Cr–Nb)N was determined from the measurements ($L_C = 62.06$ N).

4. Conclusions

The (Zr–Ti–Cr–Nb)N superhard coatings were fabricated by the vacuum-arc deposition method. The TiN fcc phase ($a = 0.243$ nm, $a_{\text{tab}} = 0.244$ nm) and tetragonal Cr_2N were formed during deposition of the investigated coatings. The hardness of the fabricated materials significantly depends on the deposition conditions, structure and phase composition. The maximum hardness $H = 43.1$ GPa was observed in the coatings with the biggest crystallite size, which were fabricated at high values of the nitrogen pressure in the chamber and substrate potential. The indenter load value exceeding the cohesive strength of coatings was $L_C = 62.06$ N.

Acknowledgments

The paper was prepared within the framework of comprehensive state program “Development of the basis for formation of multicomponent nanostructured superhard coatings with high physical and mechanical properties” (number 0112U001382) and “Physical principles of plasma technologies for complex processing of multicomponent materials and coatings” (number 0113U000137c).

References

- [1] H.E. Cheng, W.J. Lee, M. Hsu, *Thin Solid Films* **485**, 59 (2005).
- [2] J.L. Ruan, D.F. Lii, J.S. Chen, J.-L. Huang, *Ceram. Int.* **35**, 1999 (2009).
- [3] S.H. Shin, M.W. Kim, M.C. Kang, H.K. Kim, D.H. Kwon, J.S. Kim, *Surf. Coat. Technol.* **202**, 5613 (2008).
- [4] A.D. Pogrebnjak, A.G. Ponomarev, A.P. Shpak, *Phys. Usp.* **55**, 270 (2012).
- [5] A.D. Pogrebnjak, V.M. Beresnev, *Nanocoatings, Nanosystems, Nanotechnologies*, IL: Bentham Sci. Publ., Oak Park 2012, p. 147.
- [6] A.D. Pogrebnjak, V.M. Beresnev, A.A. Demianenko, *Phys. Solid State* **54**, 1882 (2012).
- [7] C.S. Sandu, R. Sanjinés, M. Benkahoul, F. Medjani, F. Lévy, *Surf. Coat. Technol.* **201**, 4083 (2006).
- [8] V.C. Kamlesh, K. Rawal, *Procedia Technol.* **14**, 430 (2014).
- [9] R. Krause-Rehberg, A.D. Pogrebnjak, V.N. Borisyuk, M.V. Kaverin, A.G. Ponomarev, M.A. Bilokur, K. Oyoshi, Y. Takeda, V.M. Beresnev, O.V. Sobol', *Phys. Met. Metallogr.* **114**, 672 (2013).
- [10] V. Ivashchenko, S. Veprek, A. Pogrebnjak, B. Postol'nyi, *Sci. Technol. Adv. Mater.* **15**, 025007 (2014).
- [11] S. Veprek, M.J.G. Veprek-Heijman, *Surf. Coat. Technol.* **202**, 5063 (2008).
- [12] N. Jiang, Y.G. Shen, H.J. Zhang, S.N. Bao, X.Y. Hou, *Mater. Sci. Eng. B* **135**, 1 (2006).
- [13] A.D. Pogrebnjak, V.M. Beresnev, O.V. Bondar, G. Abadías, P. Chartier, B.A. Postol'nyi, A.A. Andreev, O.V. Sobol', *Tech. Phys. Lett.* **40**, 215 (2014).
- [14] A.D. Pogrebnjak, A.P. Shpak, N.A. Azarenkov, V.M. Beresnev, *Phys. Usp.* **52**, 29 (2009).
- [15] R.L. Boxman, V.N. Zhitomirsky, *Rev. Sci. Instrum.* **77**, 021101 (2006).
- [16] A.D. Pogrebnjak, S. Bratushka, V.I. Boyko, I.V. Shamaninb, Yu.V. Tsvintarnaya, *Nucl. Instrum. Methods* **145**, 373 (1998).
- [17] A.D. Pogrebnjak, Yu.A. Kravchenko, S.B. Kislitsyn, Sh.M. Ruzimov, F. Noli, P. Misaelides, A. Hatzidimitriou, *Surf. Coat. Technol.* **201**, 2621 (2006).
- [18] A.D. Pogrebnjak, A.D. Mikhaliyov, N.A. Pogrebnjak, Yu.V. Tsvintarnaya, V.I. Lavrentiev, M. Iljashenko, A.N. Valyaev, S. Bratushka, A. Zecca, R. Sandrik, *Phys. Lett.* **241**, 357 (1998).
- [19] H.W. Holleck, *Surf. Coat. Technol.* **36**, 151 (1988).
- [20] G. Abadías, *Surf. Coat. Technol.* **202**, 2223 (2008).
- [21] I. Patrov, L. Hultman, J.E. Sundgen, J.E. Greene, *J. Vac. Sci. Technol.* **A10**, 265 (1992).
- [22] D. Gall, S. Kodambaka, M.A. Wall, I. Petrov, J.E. Greene, *J. Appl. Phys.* **93**, 9086 (2003).
- [23] M.K. Kazmanli, M. Urgan, A.F. Cakir, *Surf. Coat. Technol.* **167**, 77 (2003).
- [24] A.D. Pogrebnjak, A.V. Pshyk, V.M. Beresnev, B.R. Zhollybekov, *J. Frict. Wear* **35**, 55 (2014).
- [25] A.D. Pogrebnjak, A.G. Lebed, Yu.F. Ivanov, *Vacuum* **63**, 483 (2001).